Spectrochimica Acta Part A 93 (2012) 250–259

Contents lists available at SciVerse ScienceDirect

Spectrochimica Acta Part A: Molecular and Biomolecular Spectroscopy

journal homepage: www.elsevier.com/locate/saa

Developing biologically active compounds having efficient DNA binding and cleavage activity: Spectroscopic investigation

Natarajan Raman*, Sivasangu Sobha

Research Department of Chemistry, VHNSN College, Virudhunagar-626 001, India

ARTICLE INFO

Article history:
Received 19 September 2011
Received in revised form 5 March 2012
Accepted 9 March 2012

Keywords:
Schiff base metal complexes
DNA interaction
Molecular docking
Biological evaluation

ABSTRACT

A new series of novel *o*-acetoacetotoluidide derived Schiff base and its metal complexes have been synthesized and structurally characterized. Elemental analysis, magnetic and spectroscopic data suggest that the complexes have octahedral geometry. Binding of these complexes with CT-DNA has been analyzed by absorption spectra, viscosity, cyclicvoltammetry and molecular docking analysis. Detailed analysis reveals that the metal complexes intercalate into the DNA base stack as intercalators. All the metal complexes cleave the pBR322 DNA upon irradiation. Antibacterial and antifungal activities of the ligand and its metal complexes are also explored and it has been observed that the complexes exhibit excellent activity against all types of bacteria and fungi than the ligand.

1. Introduction

Recently, the development of novel metal based biologically active compounds as potential antitumor drugs is of great urgency to overcome the drug-induced cellular resistance and the efficacy of each drug against certain cancers. It is revealed from the literature that the transition metal complexes can interact non-covalently with DNA by intercalation, groove binding or external electrostatic binding [1]. Many important applications of these complexes require that they could bind to DNA in an intercalative mode. In fact, the activity of many anticancer, antimalarial and antibacterical agents finds its origin in intercalative interactions with DNA. The significance of DNA cleavage in pharmaceutical and biotechnological applications has inspired researchers to keep developing compounds that effectively cleave nucleic acid molecule.

Schiff bases play an important role in inorganic chemistry as they easily form stable complexes with most transition metal ions. The development in the field of bioinorganic chemistry has increased the interest in Schiff base complexes since it has been recognized that many of these complexes may serve as models for biologically important species [2]. The involvement of some metal ions in regulation of physiological processes has stimulated the development of metal-based therapeutics. The pharmaceutical use of complexes arises from the fact that the positively charged metal centers are favored to bind to negatively charged biomolecules such as the amino acid residues of protein constituents, ATP and nucleic acids. Moreover, the ligands can interact with biomolecules through coordinative or hydrogen bonds as well as dipole-dipole interactions [3].

The metal complexes of *o*-acetoacetotoluidide and its derivatives have been reported to show interesting biochemical properties such as antitumor, antioxidant, antifungal and antimicrobial activities [4] and laboratory uses and many industrial applications [5]. The important criteria for the development of metallodrugs as chemotherapeutic agents are the ability of the metallodrug to bring about DNA cleavage. A large number of transition metal complexes because of their redox properties, have been found to promote DNA cleavage. Transition metal complexes have been reported to bring about DNA cleavage either oxidatively or hydrolytically or photolytically [6]. The pharmacological efficiencies of metal complexes depend on the nature of the metal ions and the ligands [7]. It is declared in the literature that different ligands and different complexes synthesized from same ligands with different metal ions possess different biological properties [8]. So, there is an increasing requirement for the discovery of new compounds having antimicrobial activities. These facts prompted us to design novel transition metal complexes having DNA binding and DNA cleavage properties using *o*-acetoacetotoluitide derived Schiff base. Hence, in the present work, we report the synthesis and characterization of novel tridentate Schiff base derived from the mono-condensation of *o*-acetoacetotoluidide, hydrazine hydrate and salicylaldehyde and its transition metal(II) complexes. Information obtained from our study would be helpful in understanding the mechanism of interactions of the complexes with nucleic acid and might also be useful in the development of potential probes of DNA structure and conformation and new therapeutic reagents for some uncommon diseases.

* Corresponding author. Tel.: +91 092451 65958; fax: +91 4562 281338.
E-mail address: drn_raman@yahoo.co.in (N. Raman).

1386-1425/$ – see front matter © 2012 Elsevier B.V. All rights reserved.
doi:10.1016/j.saa.2012.03.024

2. Experimental

2.1. Reagents and instruments

All reagents *o*-acetoacetotoluidide, hydrazine hydrate, salicylaldehyde and metal(II) chlorides were of Merck products and used as supplied. Commercial solvents were distilled and then used for the preparation of ligand and its complexes. pBR322 DNA was purchased from Bangalore Genei (India). Microanalyses (C, H and N) were performed in Carlo Erba 1108 analyzer at Sophisticated Analytical Instrument Facility (SAIF), Central Drug Research Institute (CDRI), Lucknow, India. Molar conductivities in DMF (10^{-3} M) at room temperature were measured using Systronic model-304 digital conductivity meter. Magnetic susceptibility measurements of the complexes were carried out by Gouy balance using copper sulfate pentahydrate as the calibrant. The Infra-red spectra of the ligand and its complexes were obtained as KBr discs in the range 350–4500 cm^{-1} on a FT IR-8400S instrument recorded at University Science Instrumentation Center (USIC), Madurai Kamaraj University, Madurai. NMR spectra were recorded on a Bruker Avance Dry 300 FT-NMR spectrometer in $CDCl_3$ using TMS as the internal reference. FAB-MS spectra were recorded with a VGZAB-HS spectrometer at room temperature in a 3-nitrobenzylalcohol matrix. EPR spectra were recorded on a Varian E 112 EPR spectrometer in DMSO solution both at room temperature (300 K) and liquid nitrogen temperature (77 K) using TCNE (tetracyanoethylene) as the g-marker. The absorption spectra were recorded using Shimadzu model UV-1601 spectrophotometer at room temperature.

2.2. Synthesis of Schiff base ligand and its metal complexes

2.2.1. Synthesis of o-acetoacetotoluidide monohydrazone

Acetoacetotoluidide (1.91 g, 10 mmol) was dissolved in methanol (40 mL) and was added to a solution of hydrazine hydrate (0.05 g, 10 mmol) dissolved in hot methanol (10 mL). The resulting mixture was refluxed for 3 h on a water-bath. On cooling, the pale yellow compound formed was filtered, washed, dried and recrystallized from methanol.

2.2.2. Synthesis of Schiff base ligand (L)

Schematic route for synthesis of Schiff base ligand and its metal complexes is given in Scheme 1. The Schiff base has been synthesized by refluxing the reaction mixture of hot methanolic solution (30 mL) of salicylaldehyde (0.01 mol) and hot methanolic solution (30 mL) of acetoacetotoluidide monohydrazone (0.01 mol) for *ca.* 5 h with the addition of 3–4 drops of hydrochloric acid. The dark yellow color product separated was filtered and recrystallized from methanol.

2.2.3. Synthesis of metal complexes

A solution of metal(II) chloride in ethanol (2 mmol) was refluxed with an ethanol solution of the Schiff base (4 mmol) for *ca.* 2 h. Then the solution was reduced to one-third on a water bath. The solid complex precipitated was filtered off and washed thoroughly with ethanol and dried *in vacuo*.

2.3. DNA binding experiments

The interaction between metal complexes and DNA was studied using electronic absorption, viscosity and electrochemical methods. Disodium salt of calf thymus DNA was stored at 4 °C. Solution of DNA in the buffer 50 mM NaCl, 5 mM Tris–HCl (pH 7.2) in water gave a ratio 1.9 of UV absorbance at 260 and 280 nm, A_{260}/A_{280}, indicating that the DNA was sufficiently free from protein [9]. The concentration of DNA was measured using its extinction coefficient at 260 nm (6600 M^{-1}) after 1:100 dilution. Stock solutions were stored at 4 °C and used not more than 4 days. Doubly distilled water was used to prepare solutions. Concentrated stock solutions of the complexes were prepared by dissolving the complexes in DMF and diluting suitably with the corresponding buffer to the required concentration for all the experiment. Absorption titration experiments were carried out by varying the DNA concentration and maintaining the complex concentration constant. Absorbance values were recorded after each successive addition of DNA solution and equilibration (*ca.* 10 min). The absorption data were analyzed for an evaluation of the intrinsic binding constant K_b using reported procedure [10].

Electrochemical studies were carried out using CHI Electrochemical analyzer, controlled by CHI620 C software. CV measurements were performed using a glassy carbon working electrode and an Ag/AgCl reference electrode and supporting electrolyte was 50 mM NaCl, 5 mM Tris buffer (pH 7.2). All solutions were deoxygenated by purging with N_2 for 30 min prior to measurements.

Viscosity measurements at room temperature were carried out using a semi-micro dilution capillary viscometer. Each experiment was performed three times and an average flow time was calculated. Data were presented as (η/η_0) *versus* binding ratio, where η is the viscosity of DNA in presence of complex and η_0 is the viscosity of DNA alone.

2.4. Molecular modeling studies

2.4.1. Docking of metal complex with DNA

The interaction of the metal complexes with DNA was also studied by molecular modeling with special reference to docking. Extremely Fast Rigid Exhaustive Docking (FRED) version 2.1 was used for docking studies (open eye Scientific Software, Santa Fe, NM). This program generates an ensemble of different rigid body orientations (poses) for each compound conformer within the binding pocket and then passes each molecule against a negative image of the binding site. Poses clashing with this 'bump map' are eliminated. Poses surviving the bump test are then scored and ranked with a Gaussian shape function. Prior to docking, the structures of the metal complexes were constructed and geometry optimized by MM2 force field. The crystal structure of B-DNA dodecamer $d(CGCGAATTCGCG)_2$ (NDB code GDLB05), was downloaded from Protein Data Bank. Crystallographic water molecules were removed from the B-DNA. The docked poses were generated by the exhaustive search and optimization step FRED selects the single best pose from the set of candidates. This pose is then scored and the score is used to rank ligands in the output hit list. The consensus structure step allows multiple scoring functions to vote for the best docked structure in a rank-by-vote approach).

2.5. DNA photocleavage experiments

The DNA photocleavage of supercoiled pBR322 DNA (0.2 μg) to its nicked and linear form was determined by agarose gel electrophoresis in 50 mM Tris–HCl buffer (pH 7.2) containing 50 mM NaCl. For photo-induced DNA cleavage studies, the reactions were carried out under illuminated conditions using UV sources at 360 nm. After exposure to light, each sample was incubated for 1 h at 37 °C and analyzed for the photo-cleaved products using gel electrophoresis as discussed below. The inhibition reactions for the 'chemical nuclease' reactions were carried out under dark conditions by adding reagents (distamycin, 50 μM; DMSO 4 μL) prior to the addition of each complex. The inhibition reactions for the photo-induced DNA were also carried out at 360 nm using reagents sodium azide (NaN_3 100 μM;) as singlet oxygen scavenger and superoxide dismutase (10 U) prior to the addition of the complex. The samples after incubation for 1 h at 37 °C in a dark chamber were added to the loading buffer containing 25% bromophenol blue,

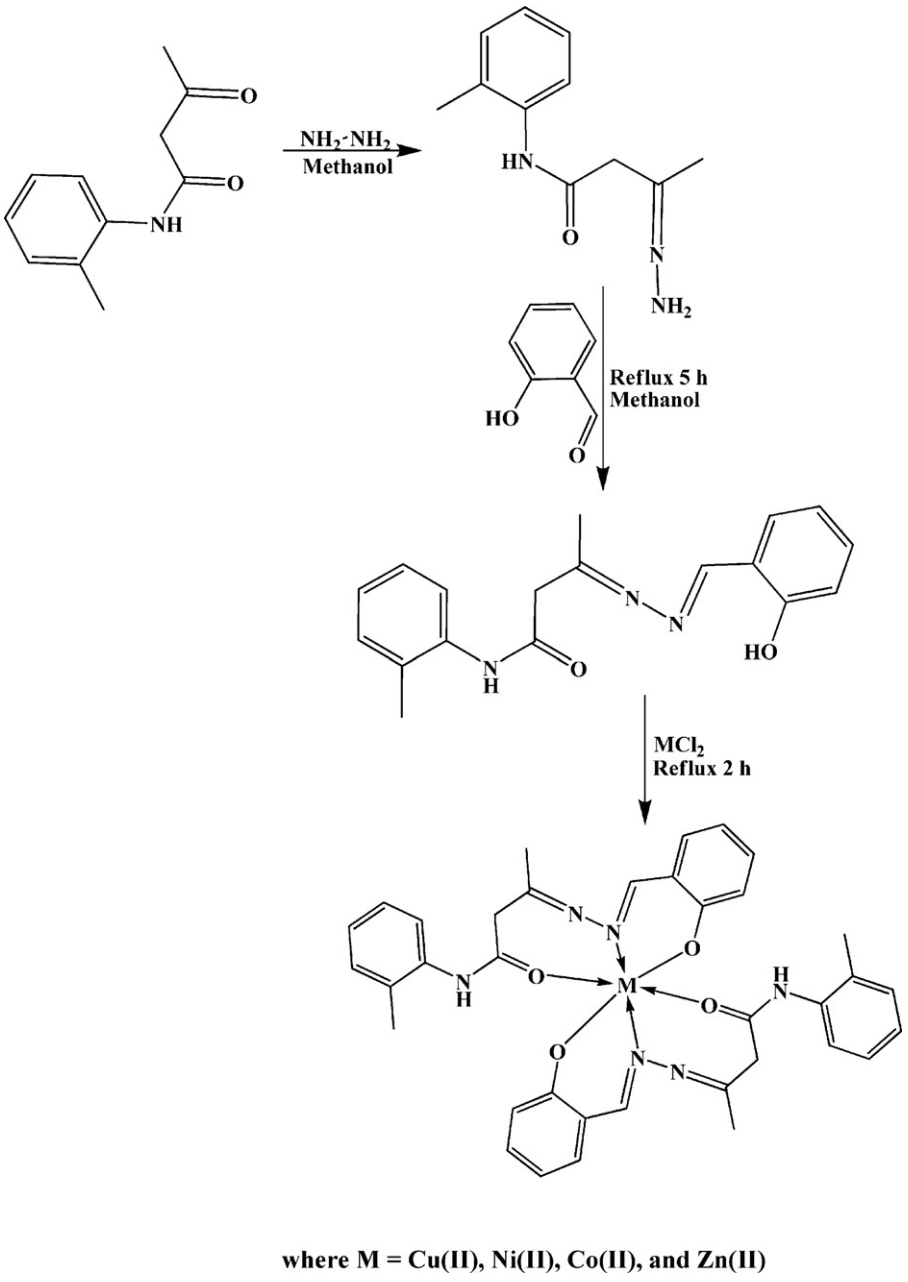

Scheme 1. Schematic route for synthesis of Schiff base ligand and its metal complexes.

0.25% xylene cyanol, 30% glycerol (3 μL) and the solution was finally loaded on 0.8% agarose gel containing 1 μg/mL ethidium bromide. Electrophoresis was carried out in a dark chamber for 3 h at 50 V in Tris-acetate-EDTA buffer. Bands were visualized by UV light and photographed.

2.6. Antimicrobial studies

Antibacterial and antifungal activity of the ligand and its metal complexes were tested *in vitro* against the bacterial species *viz.* *Staphylococcus aureus*, *Pseudomonas aeruginosa*, *Escherichia coli*, *Staphylococcus epidermidis*, *Klebsiella pneumoniae* and the fungal species *Aspergillus niger*, *Fusarium solani*, *Culvularia lunata*, *Rhizoctonia bataicola* and *Candida albicans* by the paper disk method using nutrient agar as the medium. Streptomycin was used as the standard antibacterial agent whereas nystatin was used as the standard antifungal agent. The test organisms were grown on nutrient agar medium in petri plates. Disks were prepared and applied over the long culture. The compounds were prepared in DMF and soaked in filter paper disk of 5 mm diameter and 1 mm thickness. The concentrations of ligand and the complexes used in this study were 0.01 μg/mL. The disks were placed on the previously seeded plates and incubated at 37 °C and the diameter of inhibition zone around each disk was measured after 24 h for antibacterial activity and after 74 h for antifungal activity. Growth inhibition was calculated according to Ref. [11].

3. Results and discussion

The Schiff base ligand (HL) and its Cu(II), Ni(II),Co(II) and Zn(II) complexes were synthesized and characterized by spectral and elemental analysis data. The complexes were found to be air stable. The ligand was soluble in common organic solvents but their complexes were soluble only in $CHCl_3$, DMF and DMSO.

Table 1
Analytical and physical data of Schiff base ligand and its complexes.

Compound	Yield (%)	Color	Found (calc.)%				Formula weight	($\wedge_m$)[a]	μ_{eff} (BM)
			M	C	H	N			
$[C_{18}H_{19}O_2N_3]$	81	Dark yellow	–	69.3 (69.9)	6.1 (6.1)	12.9 (13.5)	309	–	–
$[CuC_{36}H_{36}N_6O_4]$	71	Dark green	9.1 (9.3)	63.8 (64.0)	5.2 (5.3)	12.2 (12.4)	680	16.05	1.87
$[NiC_{36}H_{36}N_6O_4]$	65	Pale blue	8.2 (8.6)	63.8 (64.0)	5.1 (5.3)	12.1 (12.4)	675	11.32	3.16
$[CoC_{36}H_{36}N_6O_4]$	62	Pink	8.3 (8.7)	63.7 (64.0)	5.2 (5.3)	12.1 (12.4)	676	9.37	4.92
$[ZnC_{36}H_{36}N_6O_4]$	59	Yellow	9.1 (9.5)	62.7 (63.3)	5.3 (5.3)	11.8 (12.3)	682	18.75	Diamagnetic

[a] The unit of the molar conductance is Ω^{-1} mol^{-1} cm^2.

3.1. Elemental analysis and molar conductivity measurements

The results of elemental analysis for the metal complexes were in good agreement with the calculated values (Table 1) showing that the complexes have 1:2 metal–ligand stoichiometry of the type ML_2 wherein L acts as a tridentate ligand. The formation of these complexes may proceed according to the equation given below:

$$MCl_2{\cdot}nH_2O + 2HL \rightarrow [ML_2] + 2HCl + nH_2O$$

where, M = Cu(II), Ni (II), Co(II) and Zn(II)

The metal complexes were dissolved in DMSO and the molar conductivities of 10^{-3} M of their solution at 25 °C were measured. Table 1 shows the molar conductance values of the complexes. It is evident from the results that the chelates are found to have molar conductance values of 9.37–8.75 Ω^{-1} cm^2 mol^{-1} supporting their non-electrolytic nature.

3.2. Magnetic susceptibility and ultraviolet spectral measurements

The electronic absorbance spectrum of the ligand in ethanol showed two prominent peaks in the region 32,102 and 33,388 cm^{-1} which were assigned to intraligand charge transfer (INCT) bands. The copper(II) complex exhibited intraligand charge transfer bands at *ca.* 35,453 and 37,786 cm^{-1} and a d–d band at 14,792 cm^{-1} which was due to $^2E_g \rightarrow {}^2T_{2g}$ transition [12–15]. This d–d band transition band strongly favored a distorted octahedral geometry around the metal ion. Its magnetic moment (1.87 BM) indicates that the complex exits in monomeric nature. The electronic spectrum of the cobalt complex gave three bands at 15,060, 16,528 and 20,080 cm^{-1}, which are assigned to $^4T_{1g}(F) \rightarrow {}^4T_{2g}(F)(\upsilon_1)$, $^4T_{1g}(F) \rightarrow {}^4A_{2g}(F)(\upsilon_2)$, and $^4T_{1g}(F) \rightarrow {}^4T_{2g}(P)(\upsilon_3)$ transitions respectively [16–18]. This indicates that the complex of Co(II) is six coordinate and probably an octahedral geometry which is also supported by its magnetic susceptibility value (4.92 BM). The absorption spectrum of nickel(II) complex displayed three d–d bands at 14,636, 15,332 and 23,402 cm^{-1}, attributed to $^3A_{2g}(F) \rightarrow {}^3T_{2g}(F)(\upsilon_1)$, $^3A_{2g}(F) \rightarrow {}^3T_{1g}(F)(\upsilon_2)$ and $^3A_{2g}(F) \rightarrow {}^3T_{1g}(P)(\upsilon_3)$ transitions respectively, being characteristic of an octahedral geometry [19]. This geometry was further supported by its magnetic susceptibility value (3.16 BM). The complex of Zn(II) is diamagnetic. According to the empirical formula, an octahedral geometry is proposed for this complex.

3.3. Mass spectra

The mass spectrum of Schiff base ligand showed peak at *m*/*z* 309 corresponding to $[C_{18}H_{19}O_2N_3]$ ion. Also the spectrum exhibited peaks for the fragments at *m*/*z* 189, 120, 106 and 77 corresponding to $[C_{11}H_{13}N_2O]^+$, $[C_7H_6NO]^+$, $[C_7H_8N]^+$ and $[C_6H_5]^{+1}$ respectively. The spectra of Cu(II), Co(II), Ni(II) and Zn(II) complexes showed a molecular ion peak $[M^+]$ at *m*/*z* 680, 676, 675 and 682 respectively that are equivalent to their molecular weights. The Cu(II) complex gave a fragment ion peak with loss of one fragment of ligand peak at *m*/*z* 372. All these fragments leading to the formation of the species $[ML_2]^+$ undergo de-metallation to yield the species $[L^+]$ giving the fragment ion peak at *m*/*z* 309.

3.4. IR spectra

The IR spectra of the complexes were compared with that of the free ligand to determine the changes that might have taken place during the complexation. The IR spectra of the complexes were very similar to each other, except some slight shifts and intensity change of a few vibration bands caused by different metal ions which indicate that the complexes have similar structures. The infrared spectra of the ligand and its metal(II) complexes and important characteristic absorbance bands along with their proposed assignments are summarized in Table 2. The characteristic phenolic υ(OH) mode due to the hydroxyl group of salicylaldehyde moiety presented in the Schiff base ligand was observed at 3371 cm^{-1}. The disappearance of this band in all the complexes indicated that phenolic υ(OH) group was deprotonated upon complexation. The ligand showed its characteristic υ(C=O) band at *ca.* 1722 cm^{-1}, which was shifted to lower frequencies in the spectra of the complexes (1656–1647 cm^{-1}). In the IR spectrum of the Schiff base ligand, the band observed at 1604 cm^{-1} was shifted to lower frequency by 21–33 cm^{-1} on complexation, suggesting the coordination of the azomethine nitrogen [20]. The unaltered position of bands due to υ(NH) and υ(C=N) moiety of the acetoacetotoluidide monohydrazone in all the metal complexes indicated that these groups were not involved in coordination. The new bands in the region of 480–502 and 428–435 cm^{-1} in the spectra of the complexes were assigned to stretching frequencies of M—O and M—N bonds.

3.5. ^{1}H-NMR spectra

The ^{1}H-NMR spectra of the Schiff base and its zinc complex were recorded at room temperature in $CDCl_3$. ^{1}H-NMR spectrum of the ligand showed a singlet at δ 5.3, attributed to the phenolic —OH group of salicylaldehyde moiety presented in the Schiff base ligand. The absence of this peak noted for the zinc complex confirmed the —OH proton upon complexation. The Ph—NH— group gave singlet at δ 11.2 in the free ligand and remained unchanged in the zinc complex. It showed that the Ph—NH— group was not taking part in complexation. The ligand showed the following signals: phenyl multiplet at 6.8–8.2 δ, —CH=N at 9.8 δ, —CH_3 at 1.2-2.4 δ, —CH_2 at

Table 2
IR data of Schiff base ligand and its metal complexes.

Compound	υ_{N-H}	$\upsilon_{C=O}$	$\upsilon_{HC=N}$	$\upsilon_{C=N}$	υ_{M-N}	υ_{M-O}
$[C_{18}H_{19}O_2N_3]$	3279	1722	1604	1639	–	–
$[CuC_{36}H_{36}N_6O_4]$	3279	1656	1571	1641	428	480
$[NiC_{36}H_{36}N_6O_4]$	3283	1651	1583	1639	430	502
$[CoC_{36}H_{36}N_6O_4]$	3279	1657	1575	1639	432	489
$[ZnC_{36}H_{36}N_6O_4]$	3279	1647	1579	1639	435	495

3.1 δ. The azomethine proton (—CH=N) signal in the spectrum of the zinc complex was shifted down field compared to the free ligand, suggesting deshielding of azomethine group due to the coordination with metal ion. There was no appreciable change in all other signals of the complex.

3.6. EPR spectra

The EPR spectrum of copper complex provides information which is important in studying the metal ion environment. The EPR spectra were recorded in DMSO at LNT and at RT. The spectrum of the copper complex at RT showed one intense absorption band in the high field and was isotropic due to the tumbling motion of the molecules. However, this complex at LNT showed well resolved peaks with low field region. The copper complex exhibited the $g_{||}$ value of 2.280 and $g_{\perp}$ value of 2.046. These values indicated that the Cu(II) lies predominantly in the $d_{X^2-Y^2}$ orbital, as was evident from the value of the exchange interaction term G, estimated from the expression:

$$G = \frac{(g|| - 2)}{(g_{\perp} - 2)}$$

If $G > 4.0$, the local tetragonal axes are aligned parallel or only slightly misaligned. If $G < 4.0$, significant exchange coupling is present and the misaligned is appreciable. The observed value for the exchange interaction parameter for the copper complex ($G = 6.35$) suggests that the local tetragonal axes are aligned parallel or slightly misaligned and the unpaired electron is present in the $d_{X^2-Y^2}$ orbital. This result also indicates that the exchange coupling effects are not operative in the present complex [21].

Electron paramagnetic resonance and optical spectra have been used to determine the covalent bonding parameters for the Cu(II) ion in various environments. Since there has been wide interest in the nature of bonding parameters in the system, we adopted the simplified molecular orbital theory [9] to calculate the bonding coefficients such as α^2 (covalent in-plane σ-bonding) and β^2 (covalent in-plane π-bonding). The in-plane σ-bonding bonding parameter, α^2 is related to $g_{||}$ and $g_{\perp}$ according to the following equation:

$$\alpha^2 = \left(\frac{A_{||}}{0.036}\right) + (g_{||} - 2.0027) + \frac{3}{7}(g_{\perp} - 2.0027) + 0.04$$

If the α^2 value is 0.5, it indicates a complete covalent bonding, while the value of $\alpha^2 = 1.0$ suggests a complete ionic bonding. The observed value of α^2 (0.80) indicates that the complex has some covalent character. The in-plane π-bonding (β^2) parameter was calculated from the following equation:

$$\beta^2 = (g_{||} - 2.0027)\frac{E}{-8\lambda\alpha^2}$$

where $\lambda = -828\ cm^{-1}$ for free ion and E is the electronic transition energy of $^2E_g \rightarrow {}^2T_{2g}$. The observed value of β^2 (0.77) indicates that the σ-bonding is more covalent than the in-plane π-bonding.

Based on the above spectral and analytical data, the proposed model of Schiff base and its metal complexes is given in Supplementary file (Fig. S1).

3.7. DNA binding of the metal complexes

3.7.1. Absorption spectral aspects of DNA binding

Electronic absorption spectroscopy is usually employed to determine the binding of complexes with the DNA helix. A complex bound to DNA through intercalation is characterized by the change in absorbance (hypochromism) and red shift in wavelength, due to the intercalative mode involving a strong stacking interaction between the aromatic chromophore and the DNA base pairs. The extent of hypochromism is commonly consistent with the strength of the intercalative interaction [22].

Table 3
Electronic absorption spectral properties of Cu(II), Ni(II), Co(II) and Zn(II) complexes.

Compound	λ_{max}		Δλ (nm)	[a]H%	[b]$K_b \times 10^5$ (M^{-1})
	Free	Bound			
$[CuC_{36}H_{36}N_6O_4]$	353.2	356.8	3.6	29	2.36
$[NiC_{36}H_{36}N_6O_4]$	381.4	385.4	4.0	31	3.70
$[CoC_{36}H_{36}N_6O_4]$	320.8	324.1	3.3	26	1.28
$[ZnC_{36}H_{36}N_6O_4]$	342.1	344.8	2.7	22	1.17

[a] $H\% = [A_{free} - A_{bound})/A_{free}] \times 100\%$.
[b] K_b = Intrinsic DNA binding constant determined from the UV–vis absorption spectral titration.

The absorption spectra of the copper and nickel complexes in the absence and presence of CT-DNA are given in Figs. 1 and 2. In the UV region, the intense absorption bands observed in the metal complexes are attributed to the intra ligand π–π* transition of the coordinated groups. Addition of increasing amounts of CT-DNA resulted in hypochromism and bathochromic shift in the UV spectra of $[CuC_{36}H_{36}N_6O_4]$, $[NiC_{36}H_{36}N_6O_4]$, $[CoC_{36}H_{36}N_6O_4]$, and $[ZnC_{36}H_{36}N_6O_4]$. The hypochromism in the intraligand (IL) band reached as high as 29% at 353.2 nm with 3.6 nm red shift for $[CuC_{36}H_{36}N_6O_4]$. The absorption spectrum of $[NiC_{36}H_{36}N_6O_4]$, complex showed an intensive absorption band at 381.4 nm exhibiting hypochromism of about 31% and a bathocromic shift of 4.0 nm in 5 mM Tris–HCl, 50 mM NaCl, at pH 7.2 buffer solution, further the intense absorption band with maxima of 320.8 nm for $[CoC_{36}H_{36}N_6O_4]$ showed hypochromism of about 26% and a bathocromic shift of 3.3 nm, $[Zn_{36}H_{36}N_6O_4]$ showed a band at 342.1 nm, attributed to intraligand (IL) π–π* transition and resulting in the hypochromism of about 22% with 2.7 nm bathochromic shift. The spectral characteristics obviously suggested that the metal complexes interacted with DNA most likely through a mode that involved a stacking interaction between the aromatic chromophore and the base pairs of DNA.

The intrinsic binding constants (K_b) of the metal complexes with CT DNA were obtained by monitoring the changes in the intraligand band with increasing concentration of DNA using the following equation

$$\frac{[DNA]}{(\varepsilon_a - \varepsilon_f)} = \frac{[DNA]}{(\varepsilon_b - \varepsilon_f)} + \frac{1}{[K_b(\varepsilon_b - \varepsilon_f)]}$$

where [DNA] is the concentration of DNA in base pairs, the apparent absorption coefficients ε_a, ε_f, and ε_b are the apparent, free and bound metal complex extinction coefficients, respectively. A plot of $[DNA]/(\varepsilon_b - \varepsilon_f)$ *versus* [DNA], gave a slope of $1/(\varepsilon_b - \varepsilon_f)$ and a *Y*-intercept equal to $[K_b/(\varepsilon_b - \varepsilon_f)]^{-1}$, K_b is the ratio of the slope to the *Y*-intercept. Intrinsic binding constants of $2.36 \times 10^5\ M^{-1}$, $3.70 \times 10^5\ M^{-1}$, $1.28 \times 10^5\ M^{-1}$ and $1.17 \times 10^5\ M^{-1}$ were determined for $[CuC_{36}H_{36}N_6O_4]$, $[NiC_{36}H_{36}N_6O_4]$, $[CoC_{36}H_{36}N_6O_4]$ and $[CuC_{36}H_{36}N_6O_4]$, respectively. These values (Table 3) are comparable to the classical DNA intercalators EB (ethidium bromide, $1.4 \times 10^6\ M^{-1}$ [23] and many analogs, such as $[Ru(phen)_2(phehat)]^{2+}$ (phehat = 1,10-phenanthrolino[5,6-b]1,4,5,8,9,12-hexaazatriphenylene, $2.5 \times 10^6\ M^{-1}$ and $Ru(bpy)_2(ppd)]^{2+}$ ($1.1 \times 10^6\ M^{-1}$) [24]. The result suggests that the interaction of four metal complexes with DNA is a moderate intercalative mode.

3.7.2. Viscosity measurements

To clarify the binding mode between the metal complexes and DNA, viscosity of DNA solution containing varying amount of added complex was measured. The results indicated that the presence of the metal complex increased the viscosity of the DNA

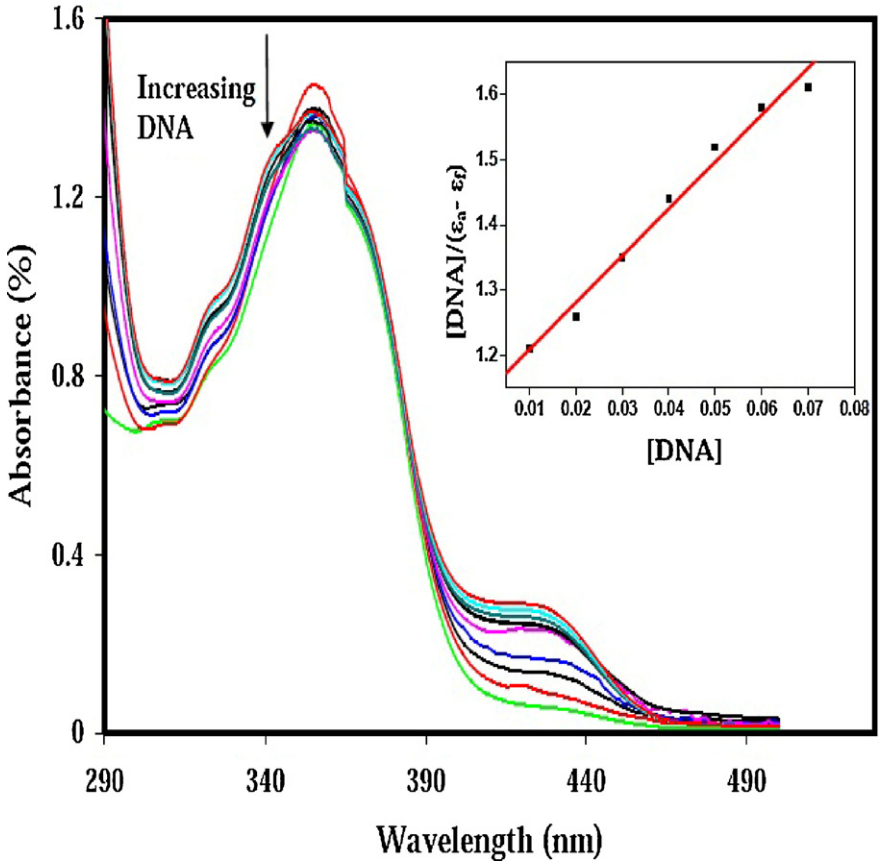

Fig. 1. Absorption spectrum of $[CuC_{36}H_{36}N_6O_4]$ complex in buffer (pH 7.2) at 25 °C upon addition of CT-DNA. Arrow indicates the changes in absorbance upon increasing the DNA concentration. Inset: plot of $[DNA]/(\varepsilon_a - \varepsilon_f)$ *versus* [DNA].

solution, as illustrated in Fig. 3. As general rule metal complexes can increase the viscosity of DNA when they intercalate into the double-stranded DNA (or) bind to the phosphate group of DNA backbone [25]. The effect of metal complexes together with ethidium bromide [EB] on the viscosity of CT-DNA is shown in Fig. 3. On increasing the amounts of metal complexes, the relative viscosity of DNA moderately increased steadily, which is similar to the behavior of ethidium bromide. The results suggest that metal complexes bind DNA with a moderate intercalative mode.

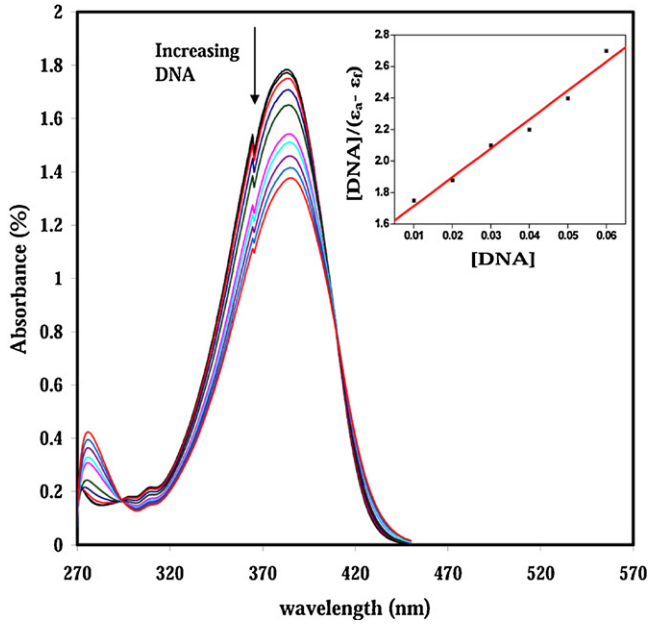

Fig. 2. Absorption spectrum of $[NiC_{36}H_{36}N_6O_4]$ complex in buffer (pH 7.2) at 25 °C upon addition of CT-DNA. Arrow indicates the changes in absorbance upon increasing the DNA concentration. Inset: plot of $[DNA]/(\varepsilon_a - \varepsilon_f)$ *versus* [DNA].

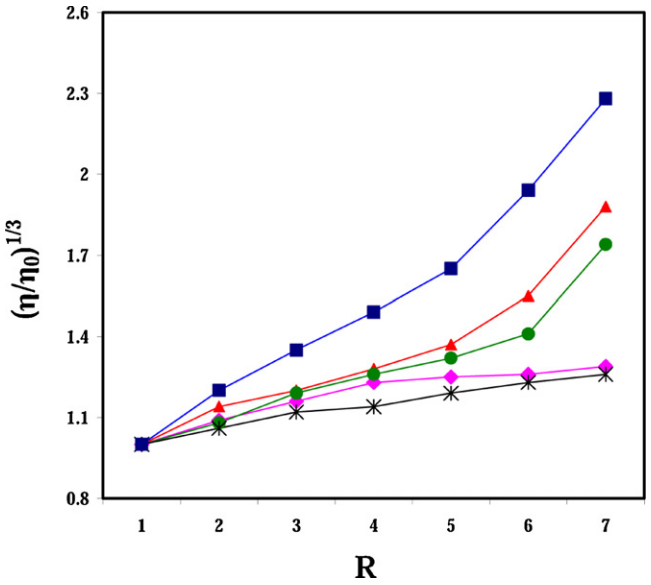

Fig. 3. Effect of increasing amounts of $[CuC_{36}H_{36}N_6O_4]$ (●), $[NiC_{36}H_{36}N_6O_4]$ (▲) $[CoC_{36}H_{36}N_6O_4]$ (♦), $[ZnC_{36}H_{36}N_6O_4]$ (✶) and [EB] (■) on the relative viscosity of DNA. *R* = [complex]/[DNA] or [EB]/[DNA].

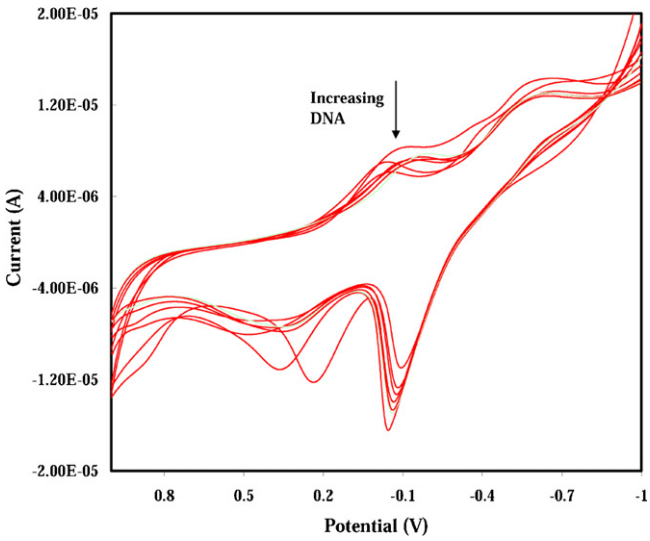

Fig. 4. Cyclic voltammogram of $[CuC_{36}H_{36}N_6O_4]$ in buffer (pH 7.2) at 25 °C in the presence of increasing amount of DNA. Arrow indicates the changes in voltammetric currents upon increasing the DNA concentration.

3.7.3. Cyclic voltammetry

The applications of electrochemical methods to the study of metallointercation and coordination of metal ion and chelates to DNA provide a useful complement to the previously used methods of investigation, such as UV–vis spectroscopy [26]. The interactions of some anticancer drugs with DNA have been studied with a variety of techniques, currently much attention have been focus to the electrochemical investigations of interactions between anticancer drugs and other DNA-targeted molecules and DNA. The cyclic voltammograms of $[CuC_{36}H_{36}N_6O_4]$ complex in the absence and in presence of varying amount of DNA is shown in Fig. 4. In the absence of CT DNA, the first redox cathodic peak appeared at −0.093 V for Cu(III) → Cu(II) [$E_{p_a} = 0.0259$ V, $E_{p_c} = -0.093$ V, ΔEp = 0.352. V and $E_{1/2}$ = 0.176 V] and in the second redox couple, the cathodic peak appeared at −0.590 V for Cu(II) → Cu(I) [$E_{p_a} = 0.034$ V, $E_{p_c} = -0.590$ V, ΔEp = 0.556 V and $E_{1/2}$ = 0.312 V]. The i_{p_a}/i_{p_c} ratio of these two redox couples is 0.92 and 1.31 respectively which indicate that the reaction of the complex on the glassy carbon electrode surface is quasi-reversible redox process. The increment addition of CT-DNA to the complex causes a positive shift in potential and a decrease in the current intensity. Among the three kinds of binding modes for small molecules to DNA, Bard has reported [27] that if $E_{1/2}$ is shifted to more negative value when small molecules interact with DNA, then the interaction mode is electrostatic binding. On the contrary, if $E_{1/2}$ is shifted to more positive value, the interaction mode is intercalative binding. Hence, it is concluded that the $[CuC_{36}H_{36}N_6O_4]$ complex could bind to DNA by intercalative mode.

For the CV behavior of $[NiC_{36}H_{36}N_6O_4]$ in the absence of DNA, the first redox couple cathodic peak appeared at −0.116 V for Ni(III) → Ni(II), ($E_{p_a} = 0.592$ V, $E_{p_c} = 0.116$ V, $\Delta E_p = -0.476$ V, and $E_{1/2} = -0.354$ V). i_{p_a}/i_{p_c} ratio of these two redox couples is approximately unity. This indicates that the reaction of the complex on the working electrode surface is quasi-reversible redox process. In the incremental addition of DNA to the complex the second cathodic peak caused a positive shift in the potential and a decrease in the current intensity. The changes of the voltammetric currents in the presence of CT DNA can be attributed to diffusion of the metal complex bound to the large, slowly diffusion DNA molecule. The changes of the peak currents observed for the complexes upon addition of CT DNA may indicate that complexes possess higher DNA binding affinity with complex. The results are similar to the above spectroscopic and viscosity data of the complexes in the presence of DNA. The cyclic voltammogram of $[NiC_{36}H_{36}N_6O_4]$ complex in the absence and in presence of varying amount of DNA is shown in Supplementary file (Fig. S2).

For Co(III) → Co(II), the redox couple cathodic peak appeared at 0.105 V in the absence of CT DNA ($E_{p_a} = 0.382$ V, $E_{p_c} = 0.105$ V, ΔE_p = 0.487 V and $E_{1/2} = -0.138$ V). The ratio of i_{p_c}/i_{p_a} is approximately unity. It indicated that the reaction of the complex on the glassy carbon electrode surface is quasi-reversible redox process. The incremental addition of CT DNA to the complex caused a positive shift in $E_{1/2}$ and a decrease in ΔEp value. The i_{p_c}/i_{p_a} values also decreased in the presence of DNA.

Finally the zinc complex showed redox cathodic peak was appearing at −0.304 V and anodic peak appearing at −0.549 V. The separation of the anodic and cathodic peak potentials is $\Delta E_p = -0.245$ V. The formal potential $E_{1/2} = -0.342$ V. The incremental addition of CT DNA to the complexes revealed that the redox couples caused a less positive shift in $E_{1/2}$ and decrease of ΔEp .The i_{p_a}/i_{p_c} values also decreased in the presence of DNA. The electrochemical parameters of the Cu(II), Ni(II), Co(II) and Zn(II) complexes are shown in Table 4. From these data it is understood that all the synthesized complexes interact with DNA through intercalating way.

3.7.4. DNA docking

The discovery and development of novel therapeutic intercalator agents for the treatment of malignancy are some of the most important goals in modern medicinal chemistry. A very interesting group in cancer therapy comprises molecules that target directly DNA. Intercalation into DNA (insertion between a pair of base pairs) is a very important process, especially with regards to the function of many anticancer drugs. The combination of spectroscopic and electrochemical methods is helpful in understanding of the interaction between DNA. In addition to this, the experiments are very useful to determine the recognition of DNA sites, and also to provide novel rational design of drugs for chemotherapy applications. Intercalation results from insertion of a planar aromatic substituent between DNA base pairs, with concomitant unwinding and lengthening of the DNA helix. The results of spectroscopic and electrochemical studies reveal that all the metal complexes are moderate intercalative compound and have good affinity for DNA. For copper, nickel, cobalt and zinc complexes, the intrinsic binding constant values (K_b) are $2.36 \times 10^5\ M^{-1}$, $3.70 \times 10^5\ M^{-1}$, $1.28 \times 10^5\ M^{-1}$ and $1.17 \times 10^5\ M^{-1}$ respectively, determined by ultraviolet spectroscopy.

The binding constant values were in the range of 10^5 per mole for all the complexes which indicated the possibility of intercalation of these complexes between the DNA base pairs. It was mainly due to more effective stacking forces between the aromatic nucleus and DNA bases. Docking experiments in the energy minimized docked structures suggested that the best possible geometry of the copper and nickel complexes was partially intercalate into the major groove as shown in Fig. 5. The intercalates were oriented parallel to the base pairs, commonly π-stacking in the major groove.

The structural analysis of docked structures gave significant details about the binding pattern of these complexes. Binding energy of docked metal complexes $[CuC_{36}H_{36}N_6O_4]$, $[NiC_{36}H_{36}N_6O_4]$, $[CoC_{36}H_{36}N_6O_4]$ and $[ZnC_{36}H_{36}N_6O_4]$ were found to be −588.70, −590.45, −585.70.6 and −573.67 kJ mol^{-1} respectively, correlating well with the experimental DNA binding values. The more negative the relative binding, the more potent the binding in between DNA and target molecules. To the best of our knowledge, the present investigation should contribute to exploring more in this area in the future.

Table 4
Electrochemical parameters for the interaction of DNA with Cu(II), Ni(II), Co(II) and Zn(II) complexes.

Compound	Redox couple	[a]$E_{1/2}$ (V)		[b]ΔE_p (V)		i_{pa}/i_{pc}
		Free	Bound	Free	Bound	
$[CuC_{36}H_{36}N_6O_4]$	Cu(III) → Cu(II)	0.176	0.366	0.352	0.428	0.92
	Cu(II) → Cu(I)	0.312	−0.320	0.556	0.487	1.31
$[NiC_{36}H_{36}N_6O_4]$	Ni(II) → Ni(I)	−0.354	−0.319	−0.476	−0.469	1.07
$[CoC_{36}H_{36}N_6O_4]$	Co(III) → Co(II)	−0.138	−0.120	−0.487	−0.490	1.30
$[ZnC_{36}H_{36}N_6O_4]$	Zn(II) → Zn(0)	−0.342	−0.401	−0.245	−0.085	0.91

[a] Data from cyclic voltammetric measurements; $E_{1/2}$ is calculated as average of anodic (E_{pa}) and (E_{pc}) peak potential $E_{1/2} = E_{pa} + E_{pc}/2$.
[b] $\Delta E_p = E_{pa} - E_{pc}$.

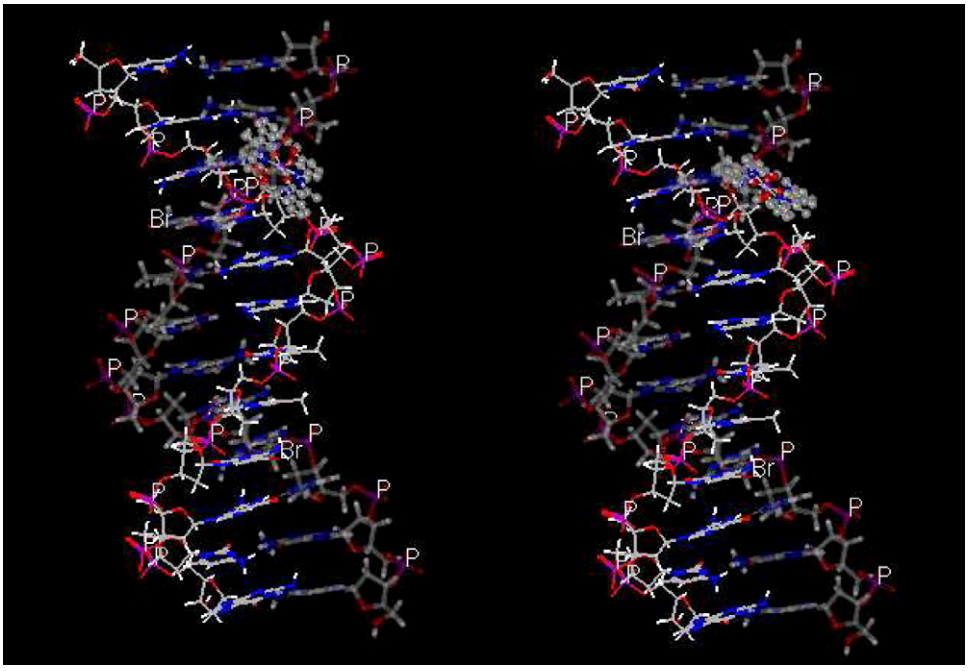

Fig. 5. Fast Rigid Exhaustive Docking molecular model of (a) copper and (b) nickel complexes partially intercalated from the major groove.

3.8. DNA photocleavage

The presence of bioactive ligand and DNA binder in the metal(II)complexes is essential for observing efficient photo-induced DNA cleavage activity. Fig. 6 shows gel electrophoresis pattern of pBR322 DNA after incubation with the four metal complexes and irradiation at 360 nm. No DNA cleavage was observed for controls in which the complex was absent (lane 0). The result indicated the importance of the metal complexes for observing the photo induced-DNA cleavage activity. All the complexes cleaved the pBR322 DNA from its supercoil form SC. The supercoil will relax to generate a slower-moving open circular form (Form II). If both strands are cleaved, a linear form (Form III) that migrates between Form I and Form II will be generated, even in the absence of inhibitors on irradiation with UV light at 360 nm.

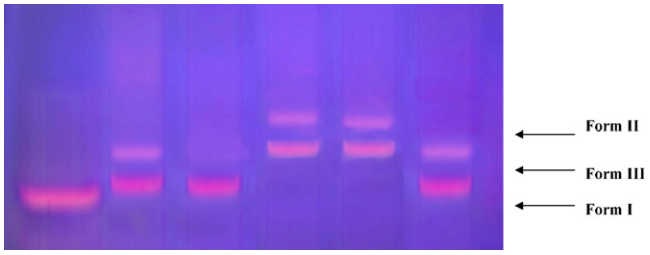

Fig. 6. Gel electrophoresis diagram showing the photocleavage of pBR322 DNA by the synthesized complexes in DMSO-Tris buffer medium on irradiation with UV light of 360 nm for 60 min: lane 1, DNA control (60 min); lane 2, DNA + ligand (60 min); lane 3; DNA + $[CuC_{36}H_{36}N_6O_4]$; DNA + $[NiC_{36}H_{36}N_6O_4]$; DNA + $[CoC_{36}H_{36}N_6O_4]$; DNA + $[ZnC_{36}H_{36}N_6O_4]$.

The mechanistic aspects of the DNA cleavage reactions involving copper and nickel complexes have been investigated at 360 nm wavelength using different inhibitors which are shown in Fig. 7a and b; the other complexes (cobalt and zinc) are given in Supplementary file (Fig. S3 and Fig. S4). In the presence of singlet oxygen quencher sodium azide the cleavage was inhibited. The cleavage of the plasmid DNA was not inhibited in the presence of hydroxyl radical scavenger like DMSO which has no apparent effect on the photo-induced DNA cleavage activity. When pBR322 DNA reacted with distamycin, a minor groove binder, the cleavage reaction was not quenched. The addition of distamycin did not inhibit the cleavage of all the complexes. While in presence of superoxide dismutase (SOD), a facile superoxide anion radical O_2^- quencher, the cleavage was improved which indicated that O_2^- might be an inhibitor in the photoactivated cleavage of the plasmid and the reducing the amount of O_2^- could improve the cleavage effect.

3.9. Antimicrobial studies

3.9.1. Antibacterial activity

The Schiff base complexes have provoked wide interest because they possess a diverse spectrum of biological and pharmaceutical

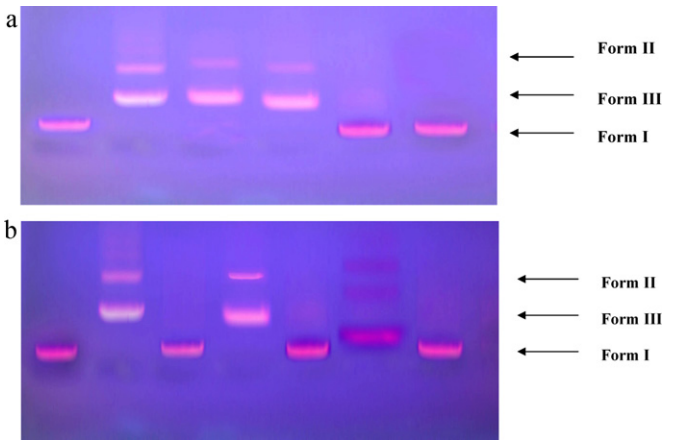

Fig. 7. (a) Photoactivated cleavage of pBR322 DNA in the presence of DNA + $[CuC_{36}H_{36}N_6O_4]$ (60 min) and different inhibitors after irradiation at 360 nm for 60 min: lane 1 DNA control (60 min); lane 2, DNA + $[CuC_{36}H_{36}N_6O_4]$ (50 μM); lane 3, DNA + $[CuC_{36}H_{36}N_6O_4]$ + sodium azide (100 μM); lane 4, DNA + $[CuC_{36}H_{36}N_6O_4]$ + SOD (1 U); lane 5, DNA + $[CuC_{36}H_{36}N_6O_4]$ + DMSO (4 μL); lane 6, DNA + $[CuC_{36}H_{36}N_6O_4]$ + distamycin (100 μM). (b) Photoactivated cleavage of pBR322 DNA in the presence of DNA + $[NiC_{36}H_{38}N_6O_4]$ (60 min) and different inhibitors after irradiation at 360 nm for 60 min: lane 1 DNA control (60 min); lane 2, DNA + $[NiC_{36}H_{36}N_6O_4]$ (50 μM); lane 3, DNA + $[NiC_{36}H_{36}N_6O_4]$ + sodium azide (100 μM); lane 4, DNA + $[NiC_{36}H_{36}N_6O_4]$ + SOD (1 U); lane 5, DNA + $[NiC_{36}H_{36}N_6O_4]$ + DMSO (4 μL); lane 6, DNA + $[NiC_{36}H_{36}N_6O_4]$ + distamycin (100 μM).

activities. The antibacterial activity of the Schiff base ligand, its metal complexes and streptomycin (as a standard compound) were tested against bacteria because bacteria could achieve resistance to antibiotics through biochemical and morphological modifications [28,29]. The organisms used in the present investigations included *S. aureus*, *P. aeruginosa*, *E. coli*, *S. epidermidis*, *K. pneumoniae*. The diffusion agar method was used to evaluate the antibacterial activity of the synthesized metal complexes.

The results of the bactericidal study of the synthesized compounds are displayed in Table 5. The zone of inhibition values obtained reflects that the Schiff base ligand has moderate activity against *S. aureus* and *E. coli* and less active against *P. aeruginosa* and *S. epidermidis*. Ligand also showed a moderate activity towards *K. pneumoniae*. The remarkable activity of the Schiff base ligand may be arise from the two imine groups which import in elucidating the mechanism of transformation reaction in biological system. All the metal complexes were found to have higher antibacterial activity against Schiff base ligand.

3.9.2. Antifungal activity

To provide in the field of bioinorganic chemistry, consequently, the metal complexes synthesized have been evaluated for their antifungal actions. The antifungal tests were carried out using the disk diffusion method. The Schiff base ligand and its metal complexes were also screened *in vitro* in order to find out the antifungal activity against *A. niger*, *F. solani*, *C. lunata*, *R. bataicola* and *C. albicans*. The results of the antifungal studies are presented in Table 6 which reveals that the metal complexes are toxic than the free ligand against the same organisms. The increase in the antifungal activity of the metal complexes inhibited multiplication process of the microbes by blocking their active sites. Such increased activity on metal chelation can be explained on the basis of Tweedy's chelation theory [30]. The chelation also increases the lipophilic nature and an interaction between the metal ion and the lipid is favored. This may be lead to the breakdown of the permeability barrier of the cell resulting in interference with the normal cell processes. While chelation is not the only factor for antimicrobial activity, it is an intricate blend of several aspects such as nature of the metal ion and the ligand, geometry of the metal complexes, lipophilicity, steric and pharmacokinetic factors [31].

Table 5
The *in vitro* antibacterial activity of Schiff base and its metal complexes (zone of inhibition in mm).

Compound	*S. aureus*	*P. aeruginosa*	*E. coli*	*S. epidermidis*	*K. pneumoniae*
$[C_{18}H_{19}N_3O_2]$	++	+	++	+	++
$[CuC_{36}H_{36}N_6O_4]$	++++	+++	+++	+++	++++
$[NiC_{36}H_{36}N_6O_4]$	++++	+++	+++	++	+++
$[CoC_{36}H_{36}N_6O_4]$	+++	++	+++	+++	++
$[ZnC_{36}H_{36}N_6O_4]$	++	++	+++	++	++
Streptomycin	++++	++++	+++	+++	+++

Streptomycin is used as the standard. DMF was used as antimicrobial inert solvent.
+++++ = Excellent activity (100% inhibition).
+++ = Good activity (60–70% inhibition).
++ = Moderate activity (30–50% inhibition).
+ = Less activity (10–20% inhibition).

Table 6
The *in vitro* antifungal activity of Schiff base and its metal complexes (zone of inhibition in mm).

Compound	*A. niger*	*F. solani*	*C. lunata*	*R. bataicola*	*C. albicans*
$[C_{18}H_{19}N_3O_2]$	++	+	+	+	+
$[CuC_{36}H_{36}N_6O_4]$	+++	++	++	++	++
$[NiC_{36}H_{36}N_6O_4]$	++++	++	++	++	+++
$[CoC_{36}H_{36}N_6O_4]$	+++	++	+++	+++	++
$[ZnC_{36}H_{36}N_6O_4]$	++	+++	++	++	+
Nystatin	++++	++	+++	+++	+++

Nystatin is used as the standard. DMF was used as antimicrobial inert solvent.
+++++ = Excellent activity (100% inhibition).
+++ = Good activity (60-70% inhibition).
++ = Moderate activity (30-50% inhibition).
+ = Less activity (10-20% inhibition).

4. Conclusion

In this paper, a novel *o*-acetoacetotoluidide derived Schiff base and its Cu(II), Ni(II), Co(II) and Zn(II) complexes have been synthesized and characterized by spectral and analytical data. The IR, electronic transition and g tensor data lead to the conclusion that the Cu(II) ion assumes a distorted octahedral geometry and the other complexes are octahedral in nature. Binding of these complexes to CT-DNA has been investigated in detail by electronic absorbance titrations, viscosity, cyclic voltammetry and molecular docking analysis. In addition, all of these metal complexes are found to promote the photocleavage of pBR322 DNA under irradiation. The singlet oxygen is suggested to be an important factor responsible for the cleavage. Hence this paper has widened the scope of developing the *o*-acetoacetotoluidide derived Schiff base and its metal complexes as promising metal based antitumor drugs. These complexes possess good biocidal (antibacterial and antifungal) activity.

Acknowledgments

The authors express their sincere thanks to the College Managing Board, Principal and Head of the Department of Chemistry, VHNSN College, Virudhunagar, India for providing necessary research facilities. They also wish to acknowledge the help rendered by Thigarajar College, Madurai with regard to computational facilities. NR thanks University Grants Commission (UGC) for financial support.

Appendix A. Supplementary data

Supplementary data associated with this article can be found, in the online version, at doi:10.1016/j.saa.2012.03.024.

References

[1] J. Jiang, X. Tang, W. Dou, H. Zhang, W. Liu, C. Wang, J. Zheng, J. Inorg. Biochem. 104 (2010) 583–591.
[2] G.G. Mohamed, M.A. Zayed, S.M. Abdallah, J. Mol. Struct. 979 (2010) 62–71.
[3] R. Olar, M. Badea, D. Marinescu, M.C. Chifiriuc, C. Bleotu, M.N. Grecu, E.E. Iorgulescu, V. Lazar, Eur. J. Med. Chem. 45 (2010) 3027–3034.
[4] K. Krishnankutty, M.B. Ummathur, J. Indian Chem. Soc. 83 (2006) 883–887.
[5] R.E. Sievers, S.B. Turnispeed, L. Huang, A.F. Laglante, Coord. Chem. Rev. 128 (1993) 285–291.
[6] G. Sathyaraj, T. Weyhermuller, B.U. Nair, Eur. J. Med. Chem. 45 (2010) 284–291.
[7] S. Delaney, M. Pascaly, P.K. Bhattacharya, K. Han, J.K. Barton, Inorg. Chem. 41 (2002) 1966–1974.
[8] K. Serbest, A. Colak, S. Güner, S. Karaböcek, Trans. Metal Chem. 26 (2001) 625–629.
[9] J. Marmur, J. Mol. Biol. 3 (1961) 208–218.
[10] A. Wolfe, G.H. Shimer, T. Meehan, Biochemistry 26 (1987) 6392–6396.
[11] A. Rahman, M.I. Choudhary, W.J. Thomsen, Bioassay Techniques for Drug Development, Harwood Academic Publishers, The Netherlands, 2001, p. 16.
[12] A.B.P. Lever, Inorganic Electronic Spectroscopy, 2nd ed., Elsevier, New York, 1968.
[13] L. Sacconi, M. Chiampolini, J. Chem. Soc. (A) 276 (1964) 1442–1454.
[14] L.N. Sharada, M.C. Ganorkar, Indian J. Chem. 27A (1988) 617–621.
[15] L. Sacconi, Trans. Metal Chem. 4 (1968) 199–298.
[16] F.A. Cotton, G. Wilkinson, C.A. Murillo, M. Bochman, Advanced Inorganic Chemistry, Sixth ed., Wiley, New York, 1999.
[17] G.G. Mohamed, Z.H. Abd, E. Wahwb, J. Thermal Anal. 73 (2003) 347–359.
[18] M.M. Omar, G.G. Mohamed, Spectrochim. Acta (Part A) 61 (2005) 929–936.
[19] G.G. Mohamed, N.A. Ibrahim, H.A.E. Attia, Spectrochim. Acta (Part A) 72 (2009) 610–615.
[20] N. Raman, S. Sobha, A. Thamaraichelvan, Spectrochim. Acta Part A 78 (2011) 888–898.
[21] N. Raman, S. Thalamuthu, J. Dhaveethuraja, M.A. Neelakandan, S. Banerjee, J. Chil. Chem. Soc. 53 (2008) 1439–1443.
[22] R.K. Ray, G.R. Kauffman, Inorg. Chim. Acta 173 (1990) 207–214.
[23] C.N. Sudhamani, H.S. Bhojya Naik, T.R. Ravikumar Naik, M.C. Prabhakara, Spectrochim. Acta Part A 72 (2009) 643–647.
[24] J.B. Lepecp, C. Paoletti, J. Mol. Biol. 27 (1967) 87–106.
[25] F. Gao, H. Chao, F. Zhou, Y.X. Yuan, B. Peng, L.N. Ji, J. Inorg. Biochem. 100 (2006) 1487–1494.
[26] Q.S. Li, R.L. Liu, J.J. Huang, P. Yang, J. Chim. Univ. (in Chinese) 21 (2000) 513–516.
[27] Q.-L. Zhang, J.-G. Liu, H. Xu, H. Li, J.-Z. Liu, H. Zhou, L.-H. Qu, L.-N. Ji, Polyhedron 20 (2001) 3049–3055.
[28] M.T. Carter, A.J. Bard, J. Am. Chem. Soc. 111 (1989) 8901–8911.
[29] G.G. Mohamed, Spectrochim. Acta Part A 64 (2006) 188–195.
[30] R. Ramesh, S. Maheswaran, J. Inorg. Biochem. 96 (2003) 457–462.
[31] M. Thankamony, K. Mohanan, Indian J. Chem. 46A (2007) 247–251.